

## Research Article

# Target Localization in Wireless Sensor Networks for Industrial Control with Selected Sensors

Zhenxing Luo,<sup>1</sup> Paul S. Min,<sup>1</sup> and Shu-Jun Liu<sup>2</sup>

<sup>1</sup> Department of Electrical and Systems Engineering, Washington University at St. Louis, St. Louis, MO 63130, USA

<sup>2</sup> College of Communication Engineering, Chongqing University, Chongqing 400044, China

Correspondence should be addressed to Zhenxing Luo; [mariolzx@gmail.com](mailto:mariolzx@gmail.com)

Received 19 January 2013; Accepted 28 May 2013

Academic Editor: Sabah Mohammed

Copyright © 2013 Zhenxing Luo et al. This is an open access article distributed under the Creative Commons Attribution License, which permits unrestricted use, distribution, and reproduction in any medium, provided the original work is properly cited.

This paper presents a novel energy-based target localization method in wireless sensor networks with selected sensors. In this method, sensors use Turbo Product Code (TPC) to transmit decisions to the fusion center. TPC can reduce bit error probability if communication channel errors exist. Moreover, in this method, thresholds for the energy-based target localization are designed using a heuristic method. This design method to find thresholds is suitable for uniformly distributed sensors and normally distributed targets. Furthermore, to save sensor energy, a sensor selection method is also presented. Simulation results showed that if sensors used TPC instead of Hamming code to transmit decisions to the fusion center, localization performance could be improved. Furthermore, the sensor selection method used can substantially reduce energy consumption for our target localization method. At the same time, this target localization method with selected sensors also provides satisfactory localization performance.

## 1. Introduction

With the advancement of hardware and software, industrial control systems (ICSs) have been widely used in many industrial areas. ICSs can use sensors to gather information about the environment or the condition of machines, and based on the information from sensors to monitor and control remote devices. Research efforts have focused on different areas of ICSs. For example, in [1], the authors discussed the security problem in ICSs. Research in [2] focused on the architecture and scheduling problem in ICSs while the authors in [3] presented an innovative control system for the industrial environment.

In many ICSs, a wireless sensor network (WSN) is laid out to control the robotics [4–6] or to track human motion [7]. Target position estimation is an essential part in these applications. There are many target localization methods available, such as direction of arrival (DOA) methods [8, 9], time-delay of arrival (TDOA) methods [10, 11], and energy-based target localization methods [12, 13]. The energy-based target localization method which uses quantized data in WSNs was presented in [12]. Compared with DOA methods and TDOA methods, energy-based target localization methods

do not require sensors to have the ability to measure the direction of arrived signals, such as in DOA methods, or require accurate synchronization among sensors, such as in TDOA methods. Therefore, energy-based target localization methods are easier to implement than the DOA methods or TDOA methods [12]. This paper focuses on energy-based target localization methods.

In energy-based target localization methods, sensors measure the signals from the target and send the measurement information to the fusion center, which uses information from the sensors to estimate the target position [12]. Usually, sensors used in WSNs have limited sources, such as energy and communication bandwidth. Therefore, saving energy and communication bandwidth are very important in WSNs.

To save energy, sensors can quantize the information about the signals from the target before sending it to the fusion center [12, 14]. There are many quantization methods, such as the nonuniform quantization method in [15] and the vector quantization method in [16]. Interested readers can refer to [17]. In the quantization scheme, thresholds are the most important parameters. In [12], a heuristic method to determine the optimum quantization thresholds

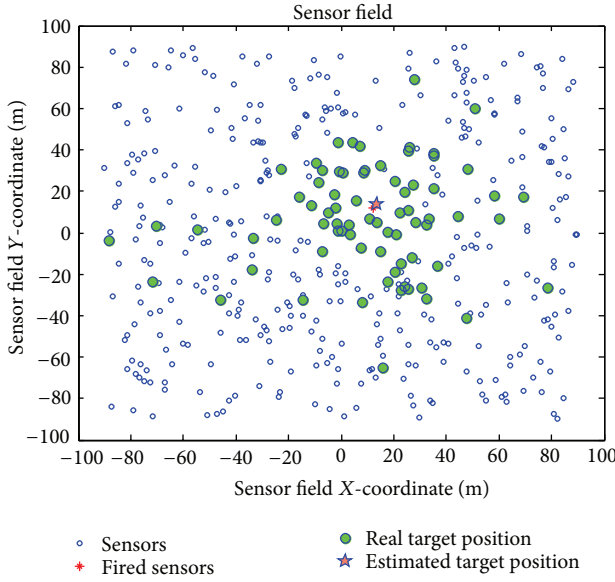


FIGURE 1: Sensor field (fired sensors are sensors having decisions other than 0).

was presented to calculate the optimum thresholds if sensor positions follow uniform distributions and the target position also follows uniform distributions. However, if the target is mostly present in a small area, Gaussian distribution can better describe the distributions of the target position. Our heuristic method can calculate optimum thresholds if the sensors are uniformly distributed and the target position follows Gaussian distributions (Figure 1).

In many applications, energy can also be saved by using a sensor selection scheme. In target tracking, [18] used an energy function and *posterior* Cramer-Rao lower bound (PCRLB) to select sensors. In [19], the authors used a modified Riccati equation approach to select sensors. In [20], a combination of PCRLB and sensor range was used to select sensors. In [21], the authors considered sensor selection when the detection probability of sensors was less than 1. More research in this area can be found in [22–25].

In target detection, [26] used a Kullback-Leibler (K-L) based approach to select sensors to maximize the K-L distance. In [27], an optimal sensor selection method in binary heterogeneous sensor networks was presented. In this paper, the K-L distance is maximized subject to cost constraints. In [28], the authors presented robust sensor selection methods to deal with uncertainties of the distribution mean.

In target estimation, if MLE is used, the Cramer-Rao lower bound (CRLB) or PCRLB can be used as the performance criterion. Then, sensors can be selected to maximize CRLB or PCRLB. In [29], sensors are selected based on PCRLB. However, in [29], several sensors were selected from all sensors. The computation cost of this selection method may be prohibitive if the total number of sensors is too large. To alleviate the computation cost, we propose a new sensor selection method in this paper.

The main contribution of this paper is a novel energy-based target localization method in WSNs with selected

sensors. In this method, sensors use Turbo Product Code (TPC) to transmit decisions to the fusion center. Moreover, the thresholds used in our target localization method are determined using a new heuristic method specifically designed for sensor position following uniform distributions and target position following Gaussian distributions. Furthermore, a sensor selection method is presented, and this selection method can significantly save sensor energy without substantially sacrificing localization performance.

The rest of this paper is organized as follows. In Section 2, an energy-based target localization method using TPC is presented. A heuristic method to determine optimum thresholds is given in Section 3, and a novel sensor selection method is presented in Section 4. The analysis of performance loss and energy saving due to sensor selection is given in Section 5. The simulation setup is presented in Section 6, and the results and analysis are provided in Section 7. The concluding remarks are made in Section 8.

## 2. Energy-Based Target Localization Method Using TPC

The energy-based target localization method using quantized data was presented in [12]. Our energy-based target localization method is based on the method in [12]. However, in our method, TPC code and sensor selection are used. Also, we only estimate two parameters.

Following the derivation in [12], acoustic signal from a target decays as distance from the target to the measurement location increases. The relation can be determined by

$$a_i^2 = \frac{G_i P_0'}{(d_i/d_0)^n}. \quad (1)$$

In (1),  $P_0'$  is the power emitted by the target measured at a reference distance  $d_0$ ,  $a_i$  is the signal amplitude from the target measured at the  $i$ th sensor,  $G_i$  is the gain of the  $i$ th sensor, which is determined by the sensor antenna, and  $n$  is the power decay exponent. The Euclidean distance between the target and the  $i$ th sensor is

$$d_i = \sqrt{(x_i - x_t)^2 + (y_i - y_t)^2}, \quad (2)$$

where  $(x_i, y_i)$  and  $(x_t, y_t)$  are the positions of sensor  $i$  and the target, respectively. It is assumed in this paper that every sensor has equal signal gain and  $d_0 = 1$ . The total number of sensors is denoted by  $N$ . Experiments showed that  $n = 2$  [12]. Therefore, (1) can be simplified as

$$a_i^2 = \frac{P_0}{d_i^2}. \quad (3)$$

Because of the presence of noise in the environment, the signal that arrived at the  $i$ th sensor will be inevitably corrupted by noises. The process can be modeled and expressed as

$$s_i = a_i + w_i, \quad (4)$$

where  $w_i$  is a Gaussian noise following the distribution  $N(0, \sigma^2)$ . To save communication bandwidth and sensor

energy,  $s_i$  is quantized [12]. In the quantization process, the  $i$ th sensor quantizes the measured signal  $s_i$  into  $m_i$  according to a set of thresholds:

$$\bar{\gamma}_i = [\gamma_{i1}, \gamma_{i2}, \gamma_{i3}, \dots, \gamma_{i(L-1)}, \gamma_{iL}]. \quad (5)$$

The quantization process used can be expressed as

$$m_i = \begin{cases} 0 & -\infty < s_i < \gamma_{i1} \\ 1 & \gamma_{i1} < s_i < \gamma_{i2} \\ 2 & \gamma_{i2} < s_i < \gamma_{i3} \\ \vdots & \vdots \\ L-2 & \gamma_{i(L-2)} < s_i < \gamma_{i(L-1)} \\ L-1 & \gamma_{i(L-1)} < s_i < \infty. \end{cases} \quad (6)$$

The probability that the transmitted decision  $m_i$  by the  $i$ th sensor takes value  $m$  can be calculated by

$$p(m_i = m | \theta) = \int_{(\eta_i - a_i)/\sigma}^{(\eta_{i+1} - a_i)/\sigma} \frac{1}{\sqrt{2\pi}} e^{-t^2/2} dt. \quad (7)$$

The channel-aware target localization method was presented in [14]. However, the authors did not use any coding method to counter communication channel errors. In our method, to minimize the effect of communication channel errors, sensors use TPC to transmit decisions to the fusion center. Previous research has focused on using Hamming code to encode decisions from sensors to the fusion center for distributed detection [30–33]. In our method, sensors use TPC to transmit decisions to the fusion center. TPC is a category of Turbo codes and can provide an efficient way to construct long codes from short linear block ones with relatively high code rates [34–36].

In TPC, BCH code is used as the component codes and iterative soft-input soft-output algorithm is used to decode rows and columns code words. Then, we can determine the relation between  $\tilde{m}_i$  and  $m$ . If the relation between  $\tilde{m}_i$  and  $m$  can be determined, we can incorporate the transition relation into the MLE framework using an approach similar to that used in [14]. The system diagram is shown in Figure 2. After the transition probabilities from  $m$  to  $\tilde{m}_i$  are determined, the probability that  $\tilde{m}_i$  assumes the value  $m$  is given by

$$p(\tilde{m}_i = m | \theta) = \sum_{m_i \in \{-1, 1\}} p(\tilde{m}_i = m | m_i) p(m_i | \theta). \quad (8)$$

In (8),  $p(m_i | \theta)$  is defined in (7). If the decision vector received at the fusion center is  $\tilde{\mathbf{M}} = [\tilde{m}_1 \ \tilde{m}_2 \ \dots \ \tilde{m}_N]^T$ , the fusion center can find  $\theta = [x_t \ y_t]^T$  to maximize

$$\ln p(\tilde{\mathbf{M}} | \theta) = \sum_{i=1}^N \ln \left[ \sum_{m_i=0}^{L-1} p(\tilde{m}_i = m | m_i) p(m_i | \theta) \right]. \quad (9)$$

The maximum likelihood estimator (MLE) tries to find  $\hat{\theta}$  to maximize

$$\hat{\theta} = \max_{\theta} \ln p(\tilde{\mathbf{M}} | \theta). \quad (10)$$

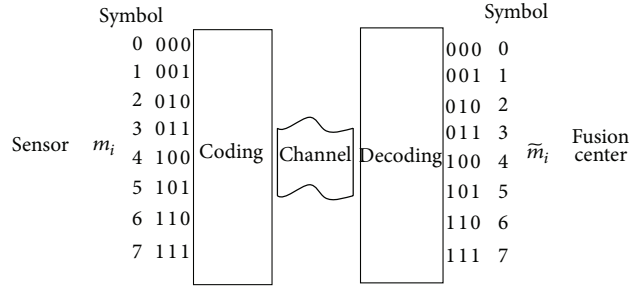


FIGURE 2: Symbol coding and decoding.

If an unbiased estimate  $\hat{\theta}$  exists, the CRLB of the estimate can be calculated by

$$E \left\{ [\hat{\theta}(\tilde{\mathbf{M}}) - \theta] [\hat{\theta}(\tilde{\mathbf{M}}) - \theta]^T \right\} \geq \mathbf{J}^{-1} \quad (11)$$

$$\mathbf{J} = -E \left[ \nabla_{\theta} \nabla_{\theta}^T \ln p(\tilde{\mathbf{M}} | \theta) \right].$$

The  $\mathbf{J}$  matrix corresponding to our two parameters estimation problem can be denoted as a 2 by 2 matrix. The process to derive the  $\mathbf{J}$  matrix is similar to the process in [14].

First,  $J(1, 1)$  is derived:

$$\begin{aligned} & \frac{\partial^2 \ln p(\tilde{\mathbf{M}} | \theta)}{\partial x_t^2} \\ &= \sum_{i=1}^N \sum_{l=1}^{L-1} - \frac{\delta(\tilde{m}_i - l)}{p^2(\tilde{m}_i | \theta)} \left[ \frac{\partial \ln p(\tilde{m}_i | \theta)}{\partial x_t} \right]^2 \\ & \quad + \frac{\delta(\tilde{m}_i - l)}{p(\tilde{m}_i | \theta)} \frac{\partial^2 p(\tilde{m}_i | \theta)}{\partial x_t^2}. \end{aligned} \quad (12)$$

Because the expectation of the second term of (12) is 0, the expectation of (12) is

$$\begin{aligned} & E \left[ \frac{\partial^2 \ln p(\tilde{\mathbf{M}} | \theta)}{\partial x_t^2} \right] \\ &= \sum_{i=1}^N \sum_{l=1}^{L-1} - \frac{1}{p^2(\tilde{m}_i | \theta)} \left[ \frac{\partial p(\tilde{m}_i | \theta)}{\partial x_t} \right]^2. \end{aligned} \quad (13)$$

In (13),  $p(\tilde{m}_i | \theta)$  is defined in (8). The derivative of  $p(\tilde{m}_i | \theta)$  with respect to  $x_t$  is

$$\frac{\partial p(\tilde{m}_i | \theta)}{\partial x_t} = \sum_{m_i=0}^{L-1} p(\tilde{m}_i | m_i) \frac{\partial p(m_i | \theta)}{\partial x_t}. \quad (14)$$

In (14),  $\partial p(m_i | \theta) / \partial x_t$  can be obtained as

$$\begin{aligned} \frac{\partial p(m_i = l | \theta)}{\partial x_t} &= \frac{\partial}{\partial x_t} \\ &\times \left[ Q\left(\frac{\eta_{il} - a_i}{\sigma}\right) - Q\left(\frac{\eta_{i(l+1)} - a_i}{\sigma}\right) \right] \\ &= \frac{-\sqrt{P_0}(x_t - x_i)}{d_i^3 \sqrt{2\pi}\sigma} \\ &\times \left( e^{-(\eta_{il} - a_i)^2 / 2\sigma^2} - e^{-(\eta_{i(l+1)} - a_i)^2 / 2\sigma^2} \right). \end{aligned} \quad (15)$$

Then, (14) can be expressed as

$$\begin{aligned} \frac{\partial p(\bar{m}_i | \theta)}{\partial x_t} &= \sum_{m_i=0}^{L-1} p(\bar{m}_i | m_i) \frac{-\sqrt{P_0}(x_t - x_i)}{d_i^3 \sqrt{2\pi}\sigma} \\ &\times \left( e^{-(\eta_{il} - a_i)^2 / 2\sigma^2} - e^{-(\eta_{i(l+1)} - a_i)^2 / 2\sigma^2} \right). \end{aligned} \quad (16)$$

Other elements of  $\mathbf{J}$  can be calculated similarly.

### 3. A Heuristic Quantization Method to Determine Optimum Threshold

Before the MLE method can be used, we have to determine an appropriate set of thresholds. Thresholds cannot be too high; otherwise, sensors will make the same decision, 0, and the MLE method cannot proceed. On the other hand, thresholds cannot be too low; otherwise, all sensors will report decision  $L - 1$  and the MLE method also cannot be implemented. In our experiments, sensors are uniformly distributed across the field. The  $X$ -coordinate of the target follows Gaussian distribution  $N(0, \sigma_x^2)$  and the  $Y$ -coordinate of the target follows Gaussian distribution  $N(0, \sigma_y^2)$ . Now the detailed steps to determine the optimum threshold are presented. The method is similar to the method used in [12].

First, we assume that the sensor position  $x_i$  follows uniform distribution

$$x_i \sim u[-a, a], \quad (17)$$

and the probability density function (PDF) of  $x_i$  is

$$f(x_i) = \frac{1}{2a}. \quad (18)$$

Similarly, we assume that the sensor position  $y_i$  also follows uniform distribution

$$y_i \in u[-a, a], \quad (19)$$

and the PDF of  $y_i$  is

$$f(y_i) = \frac{1}{2a}. \quad (20)$$

Then, we know  $-x_i$  also follows uniform distribution  $-x_i \sim u[-a, a]$  and the PDF of  $-x_i$  is

$$f(x_i) = \frac{1}{2a}. \quad (21)$$

Moreover, the target position  $x_t$  follows Gaussian distribution  $x_t \sim N(0, \sigma_x^2)$ , and the PDF of  $x_t$  is

$$f(x_t) = \frac{1}{\sqrt{2\pi}\sigma_x} e^{-x_t^2 / 2\sigma_x^2}. \quad (22)$$

Similarly, the target position  $y_t$  follows Gaussian distribution  $y_t \sim N(0, \sigma_y^2)$  and the PDF of  $y_t$  is

$$f(y_t) = \frac{1}{\sqrt{2\pi}\sigma_y} e^{-y_t^2 / 2\sigma_y^2}. \quad (23)$$

We denote  $t$  as  $t = x_i - x_t$ . Because the PDF of the sum of two independent variables is the convolution of their PDFs, we can have

$$f_T(t) = \int_{t-a}^{t+a} \frac{1}{\sqrt{2\pi}\sigma_y} e^{-\tau^2 / 2\sigma_y^2} \frac{1}{2a} d\tau. \quad (24)$$

Then, (24) can be expressed as

$$f_T(t) = \frac{1}{2a} (Q(t-a) - Q(t+a)), \quad t \in (-\infty, \infty), \quad (25)$$

in which  $Q(x)$  is defined as

$$Q(x) = \int_x^\infty \frac{1}{\sqrt{2\pi}} e^{-t^2/2} dt. \quad (26)$$

If we define  $u = (x_i - x_t)^2$ , we have  $u = t^2$ , and  $f(u)$  is

$$f(u) = \frac{1}{2\sqrt{u}} \frac{1}{2a} (Q(\sqrt{u}-a) - Q(\sqrt{u}+a)), \quad u \in (0, \infty). \quad (27)$$

If we define  $v = (x_i - x_t)^2 + (y_i - y_t)^2$ , we can have

$$\begin{aligned} f(v) &= \int_0^v \frac{1}{4a\sqrt{\tau}} (Q(\sqrt{\tau}-a) - Q(\sqrt{\tau}+a)) \\ &\times \frac{1}{4a\sqrt{v-\tau}} (Q(\sqrt{v-\tau}-a) - Q(\sqrt{v-\tau}+a)) d\tau. \end{aligned} \quad (28)$$

Because sensors have to be at least  $d_0$  meters away from the target, the minimum value of  $v$  is  $d_0^2$ . The probability that  $v$  is greater than  $d_0^2$  is

$$\alpha = 1 - \int_0^{d_0^2} f(v) dv. \quad (29)$$

Then, if  $v$  is greater or equal to  $d_0^2$ , we have

$$f_v(v | v \geq d_0^2) = \frac{1}{\alpha} f_v(v). \quad (30)$$

If we denote  $w$  as  $w = P_0/\nu$ , we can have

$$f(w) = \frac{P_0}{w^2} f_v\left(\frac{P_0}{w}\right), \quad w \in \left(0, \frac{P_0}{d_0^2}\right). \quad (31)$$

Then, (31) can be expressed as

$$\begin{aligned} f(w) &= \frac{P_0}{w^2} \frac{1}{\alpha} \\ &\times \left[ \int_0^{P_0/w} \frac{1}{4a\sqrt{\tau}} \frac{1}{4a\sqrt{(P_0/w) - \tau}} \right. \\ &\quad \times (Q(\sqrt{\tau} - a) - Q(\sqrt{\tau} + a)) \\ &\quad \times \left( Q\left(\sqrt{\frac{P_0}{w} - \tau} - a\right) \right. \\ &\quad \left. \left. - Q\left(\sqrt{\frac{P_0}{w} - \tau} + a\right) \right) d\tau \right]. \end{aligned} \quad (32)$$

If we define  $z = \sqrt{w}$ ,  $f(z)$  can be expressed as

$$f(z) = 2zf_w(z^2), \quad z \in \left(0, \sqrt{\frac{P_0}{d_0}}\right) \quad (33)$$

and finally as

$$\begin{aligned} f(z) &= 2z \frac{P_0}{z^4} \frac{1}{\alpha} \\ &\times \left[ \int_0^{P_0/w} \frac{1}{4a\sqrt{\tau}} \frac{1}{4a\sqrt{(P_0/z^2) - \tau}} \right. \\ &\quad \times (Q(\sqrt{\tau} - a) - Q(\sqrt{\tau} + a)) \\ &\quad \times \left( Q\left(\sqrt{\frac{P_0}{z^2} - \tau} - a\right) \right. \\ &\quad \left. \left. - Q\left(\sqrt{\frac{P_0}{z^2} - \tau} + a\right) \right) d\tau \right]. \end{aligned} \quad (34)$$

Now, we have the expression  $f(z)$ . According to [8], optimum threshold can be chosen so that sensors will make a decision from 0 to  $L - 1$  with equal probability. The probability that a sensor will make decision  $l$  is

$$P_l = \int_0^{\sqrt{P_0}/d_0} \left[ Q\left(\frac{\eta_l - z}{\sigma}\right) - Q\left(\frac{\eta_{(l+1)} - z}{\sigma}\right) \right] f(z) dz. \quad (35)$$

Using (35), the optimum set of thresholds can be determined.

#### 4. Sensor Selection Method

Energy is a precious resource in WSNs. Battery-powered sensors may be deployed in a remote area and replacing

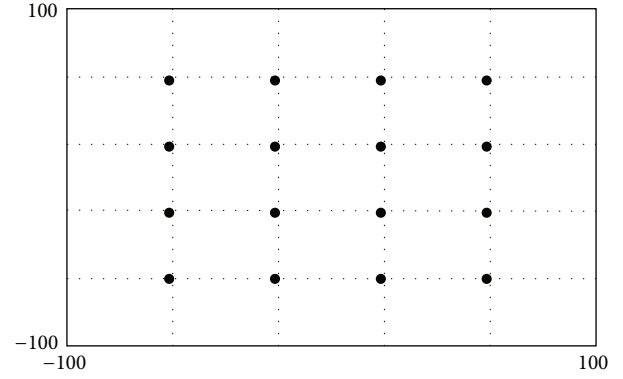


FIGURE 3: Sensor field divided into 25 sections (black points denote anchor sensors).

batteries is infeasible in many situations. Therefore, saving energy is very important in WSNs. The energy a sensor uses can be divided into three parts. The first part  $E_1$  is the energy a sensor uses to measure the signal from the target. The second part  $E_2$  is the energy a sensor uses to maintain essential functions, such as receiving information from the fusion center and keeping itself awake. The third part  $E_3$  is the energy a sensor uses to send the decisions to the fusion center. Because energy consumed in communication consists of the majority part of energy consumption, reducing  $E_3$  can significantly save sensor energy and greatly extend the operation time of a sensor. A sensor selection scheme can reduce energy consumption by choosing sensors containing more useful information and allowing those sensors to send the decisions to the fusion center while sensors containing less useful information are not allowed to send decisions to the fusion center.

In the target estimation method in [29], sensors are selected based on PCRLB from all sensors. The computation cost of this selection method may be prohibitive if the total number of sensors is large. We propose a new sensor selection method, which can alleviate the computation cost.

The steps of our method are as follows.

- (1) Divide the whole sensor field into different regions. Place  $N_0$  number of anchor sensors. For example, anchor sensors can be placed into a grid as shown in Figure 3.
- (2) Use anchor sensors and the weighted average method to estimate a coarse target position.
- (3) Use the coarse target position to choose all sensors in the region where the estimated target is located. For example, in Figure 4, region 1 will be chosen.
- (4) If the target falls into region  $M_1$ , sensors in the neighboring region, region 2, will also be chosen. If the target falls into the region  $M_2$ , sensors in the neighboring region, region 3, will also be chosen. If the target falls into  $M_3$ , sensors in all neighboring regions, region 2, region 3, and region 4, will also be chosen.

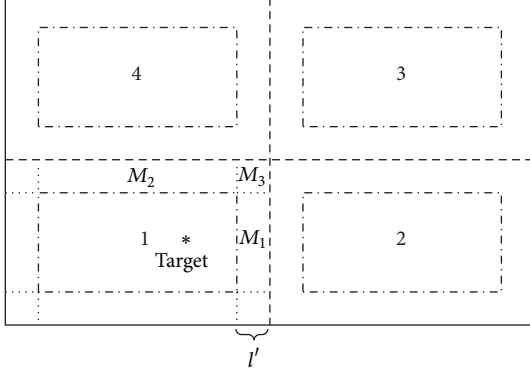


FIGURE 4: Example of sensor regions.

- (5) Chosen sensors will report decisions to the fusion center. Sensors not in chosen regions will not report decisions.

Our sensor selection method is easy to implement and circumvents the computation problem in [29]. In our method, the whole sensor field is divided into many smaller regions and a coarse target position is used to select regions in which sensors need to report their decisions to the fusion center. Therefore, our method can greatly save sensor energy.

## 5. Performance Loss and Energy Saving

Although our method can save sensor energy, the target localization performance may suffer because the fusion center does not have data from all sensors. Therefore, we also want to know the performance loss and the amount of energy saved due to sensor selection. Knowing the performance loss and how much energy was saved can help us to make the decision about when to use the sensor selection method.

**5.1. Performance Loss.** In our method, only two parameters are estimated. Therefore,  $\mathbf{J}$  is a 2 by 2 matrix:

$$\mathbf{J} = \begin{bmatrix} J_{11} & J_{12} \\ J_{21} & J_{22} \end{bmatrix}. \quad (36)$$

If the set of selected sensors is  $R_1$  and the set of nonselected sensors is  $R_2$ , then every element of  $\mathbf{J}$  can be divided into two parts. For example,

$$\begin{aligned} \mathbf{J}(1, 1) &= \sum_{i=1}^N \sum_{l=1}^{L-1} -\frac{1}{p^2(\tilde{m}_i | \theta)} \left[ \frac{\partial p(\tilde{m}_i | \theta)}{\partial x_t} \right]^2 \\ &= \sum_{i \in R_1} \sum_{l=1}^{L-1} -\frac{1}{p^2(\tilde{m}_i | \theta)} \left[ \frac{\partial p(\tilde{m}_i | \theta)}{\partial x_t} \right]^2 \\ &\quad + \sum_{i \in R_2} \sum_{l=1}^{L-1} -\frac{1}{p^2(\tilde{m}_i | \theta)} \left[ \frac{\partial p(\tilde{m}_i | \theta)}{\partial x_t} \right]^2 \end{aligned}$$

$$= \mathbf{J}^1(1, 1) + \mathbf{J}^2(1, 1)$$

$$\mathbf{J} = \mathbf{J}^1 + \mathbf{J}^2 = \begin{bmatrix} J_{11}^1 & J_{12}^1 \\ J_{21}^1 & J_{22}^1 \end{bmatrix} + \begin{bmatrix} J_{11}^2 & J_{12}^2 \\ J_{21}^2 & J_{22}^2 \end{bmatrix}. \quad (37)$$

Similarly, other elements can also be expressed as two parts: fisher information contributed by selected sensors and fisher information contributed by nonselected sensors. The performance loss is due to loss of Fisher information from nonselected sensors. However, this method to determine performance loss is valid only if the target is at a fixed position. If the target is randomly distributed, root-mean-square (RMS) estimation errors can be used to show the performance loss. We can compare the RMS estimation errors provided by the MLE method using data from all sensors and the RMS estimation errors provided by the MLE method using data only from chosen sensors.

**5.2. Energy Saving.** It is assumed that each region has the same size and the same  $M_1$ ,  $M_2$ , and  $M_3$ . We use  $A$  to denote the area of each region,  $A_1$  to denote the area of  $M_1$ ,  $A_2$  to denote the area of  $M_2$ , and  $A_3$  to denote the area of  $M_3$ . Also, we assume that the fusion center is far away from the sensors. Therefore, the difference in sensor positions is not important and each sensor will consume the same amount of energy to send decisions to the fusion center. This energy is denoted by  $e_1$ , which can be calculated by

$$e_1(m, d_{f,i}) = E_{\text{elec}} \times m + \epsilon_{\text{amp}} \times m \times d_{f,i}^2, \quad (38)$$

where  $E_{\text{elec}} = 50 \text{ uJ/bit}$ ,  $\epsilon_{\text{amp}} = 100 \text{ nJ/bit/m}^2$ , and  $d_{f,i}$  is the distance between the  $i$ th sensor and the fusion center [37].

The total number of sensors in the sensor field is  $N$ , and we assume that each region has the same number of sensors,  $N_{\text{region}}$ . Then, the probability that the target is located in region  $M_1$  is  $A_1/A$ , the probability that the target is located in  $M_2$  is  $A_2/A$ , and the probability that the target is located in  $M_3$  is  $A_3/A$ . We assume that the target mostly concentrates in the center of the field, and in the center of the field, the target is almost uniformly distributed. In each region, there are two  $M_1$  areas, two  $M_2$  areas, and four  $M_3$  areas. If the target is located in  $M_1$ , the neighboring region is also activated. Similarly, If the target is located in  $M_2$ , the neighboring region is also activated. If the target is located in  $M_3$ , the other three neighboring regions are also activated. Therefore, the energy sensors consume to transmit decisions can be expressed as

$$\begin{aligned} E_4 &= e_1 * N_{\text{region}} \\ &\quad * \left( \frac{A - 2A_1 - 2A_2 - 4A_3}{A} + 4\frac{A_1}{A} + 4\frac{A_2}{A} + 16\frac{A_3}{A} \right). \end{aligned} \quad (39)$$

Without sensor selection, the energy consumed by sensors to transmit decisions is

$$E_5 = N_{\text{total}} * N_{\text{field}} * e_1. \quad (40)$$

Now, we know the performance loss and energy saved. Using the information about the performance loss and energy saved, we can strike the balance between performance loss and energy saving. Also, a multi-objective optimization method can be used to jointly optimize performance loss and energy saving.

## 6. Simulation Setup

**6.1. TPC Encoding and Decoding.** If sensors use TPC to transmit decisions to the fusion center, localization performance can be improved due to lower bit error probability. For comparison purposes, simulations were run to show the localization performance when TPC code was used and the localization performance when Hamming code was used. In simulations, each sensor quantized the received signal into 3 bits data. In hamming code, we used (7, 4, 3) Hamming code. In TPC, we used BCH (32, 26) codes as the component code, so the rate of TPC was  $(26/32) \times (26/32) = 0.67$ . A highly efficient iterative decoding algorithm, ALD-FBBA, is used at the receiver side. ALD-FBBA can provide good performance with low complexity. If communication channel SNR was 7 dB, the bit error probability was 0.0077 for Hamming code and 0.0002 for TPC code. We calculated the decision transition matrix using the bit error probability. Using the decision transition matrix corresponding to Hamming code and the decision transition matrix corresponding to the TPC, we compared the effect of coding on localization performance. We set  $(x_t, y_t) = (0, 0)$ ,  $a = 90$ , and  $P_0 = 8000$ . We used 480 sensors and varied  $\sigma$  to see the effect of signal noise on localization performance. 100 Monte Carlo simulations were used to calculate RMS errors. The thresholds were set to

$$\bar{y}_i = [-\infty, 0.917, 1.017, 1.116, 1.25, 1.45, 1.79, 2.6, \infty]. \quad (41)$$

We define RMS location error as

$$\Delta = \text{RMS errors}(\hat{x}_t - x_t) + \text{RMS errors}(\hat{y}_t - y_t) \quad (42)$$

and used  $\Delta$  as performance criterion.

**6.2. Performance Loss and Energy Saving.** We used random target locations in the simulation. Therefore, we used  $\Delta$  in (42) as the performance criterion. Energy saving can be easily calculated by comparing  $E_4$  in (39) and  $E_5$  in (40). In this simulation, sensors were uniformly distributed in the sensor field with  $a = 90$  and the target position followed Gaussian distribution with  $x_t \sim N(0, 36^2)$  and  $y_t \sim N(0, 36^2)$ . We set  $\sigma = 1$ ,  $P_0 = 8000$ , and assumed perfect communication channels. We divided the sensor field into 25 regions as shown in Figure 3 and set the  $l'$  in Figures 2 to 4. The whole sensor field had 480 sensors. Each sensor used the same amount of energy,  $E_1 + E_2 = 6e - 3$  J, every second whether it was selected or not. Selected sensors made 10,000 sets of transmission every second. We assumed that the distances from the sensors to the fusion center were the same, 1,000 meters. The optimum thresholds for this setting were

$$\bar{y}_i = [-\infty, 0, 0.54, 0.96, 1.35, 1.76, 2.27, 3.31, \infty]. \quad (43)$$

The optimum thresholds were used in the simulations.

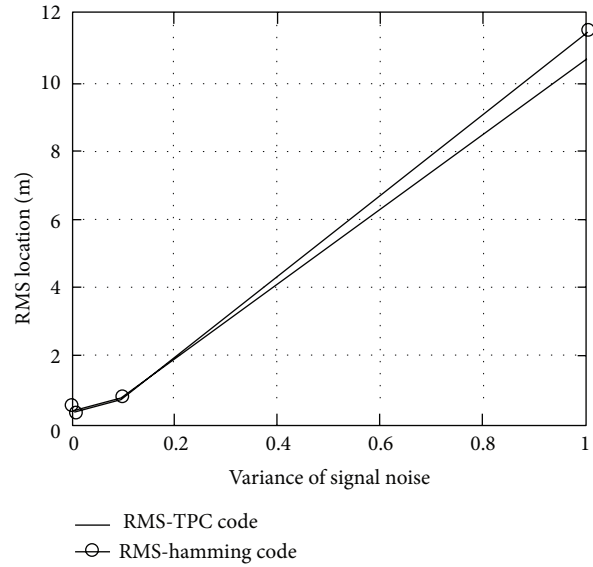


FIGURE 5: RMS location errors as a function of the variance of signal noise (RMS location errors were defined in (42), and the variance of signal noise is  $\sigma^2$ ).

## 7. Results and Analysis

**7.1. TPC Encoding and Decoding.** Figure 5 shows that RMS location error as a function of the variance of signal noise. The RMS location error increased as the variance of signal noise increased. Moreover, the RMS location errors given by the MLE method using TPC were lower than the RMS location errors given by Hamming code. This means that if the MLE method uses TPC, the localization performance will be better. The threshold set used in this simulation was presented in (41), which was an optimum threshold set determined by the heuristic method. To determine the optimum set of thresholds, we used  $a = 90$  and  $\sigma_x^2 = \sigma_y^2 = 0.001^2$ . The variance of  $x_t$  and the variance of  $y_t$  were very small. That means the target rarely moved to another position and was almost fixed at position (0,0). Therefore, the threshold set determined using these parameters was valid for our simulation where  $(x_t, y_t) = (0, 0)$ . Moreover, when the sensors used the optimum threshold set in (41), the numbers of sensors making each particular decision were almost the same (Figure 6). The results in Figure 6 validated the optimum set of thresholds calculated using (35).

**7.2. Performance Loss and Energy Saving.** Simulation results showed that using the setting described in Section 6.2, we had  $\Delta_{\text{with\_selection}} = 8.3031$  and  $\Delta_{\text{without\_selection}} = 3.9825$ . The difference between  $\Delta_{\text{with\_selection}}$  and  $\Delta_{\text{without\_selection}}$  is performance loss due to sensor selection. As for energy saving, if our sensor selection method was used, the energy consumption of all sensors was  $E_{\text{selection}} = 28.4928$  J per second. If our sensor selection was not used, the energy consumption of all sensors was  $E_{\text{without\_selection}} = 483.12$  J per second. We can see that the sensor selection method

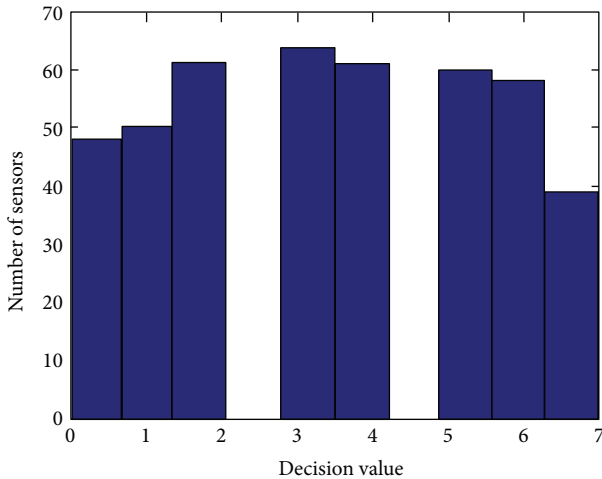


FIGURE 6: Number of sensors as a function of decision value.

can greatly reduce energy consumption while sacrificing a moderate degree of performance.

## 8. Conclusion

In this paper, a novel energy-based target localization method with selected sensors was presented. It is well known that communication channel errors can degrade the energy-based target localization methods. Our new target localization method uses TPC to counter communication channel errors. Simulation results showed that the target localization method using TPC can provide better localization performance than the target localization method using hamming code. Moreover, the sensor selection method used can save energy without great performance degradation as demonstrated by simulation results. Furthermore, if sensors use the optimum thresholds determined by the heuristic method, there will be about the same number of sensors making each particular decision. Overall, the new energy-based target localization method with selected sensors can achieve good localization performance with less energy consumption.

## Acknowledgment

The authors want to thank Bingchao Liu from the School of Information and Communication Engineering, Beijing University of Posts and Telecommunications, China, for providing numerical parameters about Hamming code and TPC code.

## References

- [1] P. Jie and L. Li, "Industrial control system security," in *Proceedings of the 3rd International Conference on Intelligent Human-Machine Systems and Cybernetics (IHMSC '11)*, pp. 156–158, Zhejiang, China, August 2011.
- [2] J. Wang, H. Wang, H. Yu, and A. Xu, "Research of architecture and scheduling for wireless industrial control system," in *Proceedings of the IEEE International Conference on Information Acquisition (ICIA '06)*, pp. 936–940, Shandong, China, August 2006.
- [3] M. Foursa, D. D'Angelo, and R. Narayanan, "Innovative control system for industrial environment," in *Proceedings of the 4th International Conference on Autonomic and Autonomous Systems (ICAS '08)*, pp. 82–87, March 2008.
- [4] B. Song, G. Tian, G. Li, F. Zhou, and D. Liu, "ZigBee based wireless sensor networks for service robot intelligent space," in *Proceedings of the International Conference on Information Science and Technology (ICIST '11)*, pp. 834–838, Nanjing, China, March 2011.
- [5] G. Mester, "Wireless sensor-based control of mobile robots motion," in *Proceedings of the 7th International Symposium on Intelligent Systems and Informatics (SISY '09)*, pp. 81–84, Subotica, Serbia, September 2009.
- [6] G. Mester, I. Matijevics, T. Szepe, and J. Simon, *Application and Multidisciplinary Aspects of Wireless Sensor Networks: Concepts, Integration, and Case Studies*, Springer, New York, NY, USA, 2010.
- [7] S. Zhang, W. Xiao, J. Gong, and Y. Yin, "A novel human motion tracking based on wireless sensor network," *International Journal of Distributed Sensor Networks*, vol. 2013, Article ID 636052, 7 pages, 2013.
- [8] X. Li and J. Huang, "Bayesian high resolution DOA estimator based on importance sampling," in *Proceedings of the Oceans 2005—Europe*, pp. 611–615, June 2005.
- [9] R. Sanudin, N. H. Noordin, A. O. El-Rayis, N. Haridas, A. T. Erdogan, and T. Arslan, "Analysis of DOA estimation for directional and isotropic antenna arrays," in *Proceedings of the 7th Loughborough Antennas and Propagation Conference (LAPC '11)*, pp. 1–4, Loughborough, UK, November 2011.
- [10] M. Sun and K. C. Ho, "An asymptotically efficient estimator for TDOA and FDOA positioning of multiple disjoint sources in the presence of sensor location uncertainties," *IEEE Transactions on Signal Processing*, vol. 59, no. 7, pp. 3434–3440, 2011.
- [11] K. C. Ho, "Bias reduction for an explicit solution of source localization using TDOA," *IEEE Transactions on Signal Processing*, vol. 60, no. 5, pp. 2101–2114, 2012.
- [12] R. X. Niu and P. K. Varshney, "Target location estimation in sensor networks with quantized data," *IEEE Transactions on Signal Processing*, vol. 54, no. 12, pp. 4519–4528, 2006.
- [13] X. Sheng and Y.-H. Hu, "Maximum likelihood multiple-source localization using acoustic energy measurements with wireless sensor networks," *IEEE Transactions on Signal Processing*, vol. 53, no. 1, pp. 44–53, 2005.
- [14] O. Ozdemir, R. Niu, and P. K. Varshney, "Channel aware target localization with quantized data in wireless sensor networks," *IEEE Transactions on Signal Processing*, vol. 57, no. 3, pp. 1190–1202, 2009.
- [15] M. Hagiwara, T. Kitayabu, H. Ishikawa, and H. Shirai, "Delta-sigma modulator with non-uniform quantization," in *Proceedings of the IEEE Radio and Wireless Symposium (RWS '11)*, pp. 351–354, Phoenix, AZ, USA, January 2011.
- [16] T. K. Grönfors and N. S. Päivinen, "Comparison of vector quantization methods for medical fidelity preserving lossy compression of EMG signals," in *Proceedings of the International Conference on Computational Intelligence for Modelling, Control and Automation (CIMCA '05) and International Conference on Intelligent Agents, Web Technologies and Internet Commerce (IAWTIC '05)*, pp. 1107–1113, Vienna, Austria, November 2005.

- [17] B. Widrow and I. Kollár, *Quantization Noise: Roundoff Error in Digital Computation, Signal Processing, Control, and Communications*, Cambridge University Press, Cambridge, UK, 2008.
- [18] H. Ma, "Sensing nodes selection scheme for distributive target tracking in wireless sensor networks," in *Proceedings of the 37th Annual Conference of the IEEE Industrial Electronics Society (IECON '11)*, pp. 2164–2169, Melbourne, Australia, November 2011.
- [19] U. Ramdas and F. Absil, "Sensor selection: the modified Riccati equation approach compared with other selection schemes," in *Proceedings of the 10th International Conference on Information Fusion (FUSION '07)*, Quebec, Canada, July 2007.
- [20] Z. Liu, J. Wang, and H. Wang, "PCRLB-based cluster selection for target tracking in wireless sensor networks," in *Proceedings of the 3rd International Conference on Cyber-Enabled Distributed Computing and Knowledge Discovery (CyberC '11)*, pp. 83–87, Beijing, China, October 2011.
- [21] U. D. Ramdas and F. Bolderheij, "Performance-based sensor selection for optimal target tracking," in *Proceedings of the 12th International Conference on Information Fusion (FUSION '09)*, pp. 1687–1694, July 2009.
- [22] F. R. Armaghani, I. Gondal, and J. Kamruzzaman, "Dynamic sensor selection for target tracking in wireless sensor networks," in *Proceedings of the IEEE 74th Vehicular Technology Conference (VTC Fall '11)*, San Francisco, CA, USA, September 2011.
- [23] Z. Liu and J. Wang, "PCRLB-based optimal sensor selection for maneuvering target tracking," in *Proceedings of the 7th International Conference on Wireless Communications, Networking and Mobile Computing (WiCOM '11)*, Wuhan, China, September 2011.
- [24] S. Zhang, W. Xiao, M. H. Ang Jr., and C. K. Tham, "IMM filter based sensor scheduling for maneuvering target tracking in wireless sensor networks," in *Proceedings of the International Conference on Intelligent Sensors, Sensor Networks and Information Processing (ISSNIP 07)*, pp. 287–292, Melbourne, Australia, December 2007.
- [25] M. R. Zoghi and M. H. Kahaei, "Sensor selection for target tracking in WSN using modified INS algorithm," in *Proceedings of the 3rd International Conference on Information and Communication Technologies: From Theory to Applications (ICTTA '08)*, Damascus, Syria, April 2008.
- [26] V. Srivastava, K. Plarre, and F. Bullo, "Adaptive sensor selection in sequential hypothesis testing," in *Proceedings of the 50th IEEE Conference on Decision and Control and European Control Conference (CDC-ECC '11)*, pp. 6284–6289, Orlando, FL, USA, December 2011.
- [27] M. Lázaro, M. Sánchez-Fernández, and A. Artes-Rodríguez, "Optimal sensor selection in binary heterogeneous sensor networks," *IEEE Transactions on Signal Processing*, vol. 57, no. 4, pp. 1577–1587, 2009.
- [28] D. Bajović, B. Sinopoli, and J. Xavier, "Sensor selection for event detection in wireless sensor networks," *IEEE Transactions on Signal Processing*, vol. 59, no. 10, pp. 4938–4953, 2011.
- [29] E. Maşazade, R. X. Niu, P. K. Varshney, and M. Keskinöz, "Energy aware iterative source localization for wireless sensor networks," *IEEE Transactions on Signal Processing*, vol. 58, no. 9, pp. 4824–4835, 2010.
- [30] T.-Y. Wang, Y. S. Han, B. Chen, and P. K. Varshney, "A combined decision fusion and channel coding scheme for distributed fault-tolerant classification in wireless sensor networks," *IEEE Transactions on Wireless Communications*, vol. 5, no. 7, pp. 1695–1705, 2006.
- [31] C. Yao, P.-N. Chen, T.-Y. Wang, Y. S. Han, and P. K. Varshney, "Performance analysis and code design for minimum hamming distance fusion in wireless sensor networks," *IEEE Transactions on Information Theory*, vol. 53, no. 5, pp. 1716–1734, 2007.
- [32] T.-Y. Wang, Y. S. Han, and P. K. Varshney, "Fault-tolerant distributed classification based on non-binary codes in wireless sensor networks," *IEEE Communications Letters*, vol. 9, no. 9, pp. 808–810, 2005.
- [33] T.-Y. Wang, Y. S. Han, P. K. Varshney, and P.-N. Chen, "Distributed fault-tolerant classification in wireless sensor networks," *IEEE Journal on Selected Areas in Communications*, vol. 23, no. 4, pp. 724–734, 2005.
- [34] J. Fang, F. Buda, and E. Lemois, "Turbo product code: a well suitable solution to wireless packet transmission for very low error rates," in *Proceedings of the 2nd International Symposium on Turbo Codes and Related Topics*, pp. 101–111, 2000.
- [35] R. M. Pyndiah, "Near-optimum decoding of product codes: block turbo codes," *IEEE Transactions on Communications*, vol. 46, no. 8, pp. 1003–1010, 1998.
- [36] M. P. C. Fossorier and S. Lin, "Soft-input soft-output decoding of linear block codes based on ordered statistics," in *Proceedings of the IEEE Global Telecommunications Conference (GLOBECOM '98)*, pp. 2828–2833, November 1998.
- [37] W. R. Heinzelman, A. Chandrakasan, and H. Balakrishnan, "Energy-efficient communication protocol for wireless microsensor networks," in *Proceedings of the 33rd Annual Hawaii International Conference on System Sciences*, pp. 10–20, January 2000.

